Flight behavior of the rhinoceros beetle *Trypoxylus dichotomus* during electrical nerve stimulation

Flight behavior of the rhinoceros beetle *Trypoxylus dichotomus* during electrical nerve stimulation

Tien Van Truong[1], Doyoung Byun[2,7], Laura Corley Lavine[3], Douglas J Emlen[4], Hoon Cheol Park[5] and Min Jun Kim[6]

[1] Department of Aerospace Information Engineering, Konkuk University, Seoul 143-701, Korea
[2] Department of Mechanical Engineering, Sungkyunkwan University, Suwon 440-746, Korea
[3] Department of Entomology, Washington State University, Pullman, WA 99164, USA
[4] Division of Biological Sciences, University of Montana, Missoula, MT 59812, USA
[5] Department of Advanced Technology Fusion, Konkuk University, Seoul 143-701, Korea
[6] Department of Mechanical Engineering and Mechanics, Drexel University, Philadelphia, PA 19104, USA

E-mail: dybyun@skku.edu

Abstract

Neuronal stimulation is an intricate part of understanding insect flight behavior and control insect itself. In this study, we investigated the effects of electrical pulses applied to the brain and basalar muscle of the rhinoceros beetle (*Trypoxylus dichotomus*). To understand specific neuronal stimulation mechanisms, responses and flight behavior of the beetle, four electrodes were implanted into the two optic lobes, the brain's central complex and the ventral nerve cord in the posterior pronotum. We demonstrated flight initiation, turning and cessation by stimulating the brain. The change undergone by the wing flapping in response to the electrical signal was analyzed from a sequence of images captured by a high-speed camera. Here, we provide evidence to distinguish the important differences between neuronal and muscular flight stimulations in beetles. We found that in the neural potential stimulation, both the hind wing and the elytron were suppressed. Interestingly, the beetle stopped flying whenever a stimulus potential was applied between the pronotum and one side of the optic lobe, or between the ventral nerve cord in the posterior pronotum and the central complex. In-depth experimentation demonstrated the effective of neural stimulation over muscle stimulation for flight control. During electrical stimulation of the optic lobes, the beetle performed unstable flight, resulting in alternating left and right turns. By applying the electrical signal into both the optic lobes and the central complex of the brain, we could precisely control the direction of the beetle flight. This work provides an insight into insect flight behavior for future development of insect-micro air vehicle.

S Online supplementary data available from stacks.iop.org/BB/7/036021/mmedia

(Some figures may appear in colour only in the online journal)

---

[7] Author to whom any correspondence should be addressed.

1. Introduction

Electrical control of the locomotory patterns of animals is an active area of research. In short, this entails inducing artificial stimulation of an organism's nervous system in order to replicate and study naturally occurring processes of the organism. Several methods, such as direct electrical stimulation of muscles, electrical stimulation of neurons, projection of pheromones and stimulation of insect sensory cells, are used to control an insect's ground and flight movements [1]. For example, neural stimulation of the brain has been demonstrated to control the locomotion of a cockroach and a rat [2–4].

Insects are particularly well adapted for flight. The excellent flight performance of insects is primarily attributable to their large power-to-weight ratio [5]. Insects are capable of long-distance flight, hovering and swift maneuvering [6, 7]. Many studies have been conducted in order to understand the aerodynamic characteristics of insect flight [8–11] with the goal of developing micro air vehicles (MAVs) that will mimic an insect's flight ability [12–18]. An insect may be considered as an autonomous flying machine exhibiting better aerodynamic performance than any existing flying machine [19]. Controlling insect flight requires not only triggering flight initiation but also flight cessation behaviors, as well as controlling flight orientation [20]. Recent reports discuss methods of controlling insect flight including muscle heating [21], chemical injection [22] and electrical stimulation [22–27]. In these studies, electrical stimulation exhibited low power consumption, easy integration with electronic systems and immediate response times [27]. However, quantitative studies examining the flight dynamics of an insect under the control of neural stimulation have not been previously conducted in any insect species.

Direct electrical stimulation of muscles and neurons had been used for controlling insects traveling in flight and on ground. Sato *et al* demonstrated the remote control of a *Mecynorrhinatorquata* beetle via neural and muscular stimulations [24, 25]. Flight initiation and cessation were controlled using two electrodes implanted into the beetle's brain to stimulate the optic lobes. Control of turning was achieved through direct muscular stimulation of either right or left basalar flight muscles. However, specific neuronal mechanisms of beetles have not been thoroughly studied for the purpose of applying control functions to beetle flight initiation, cessation and turns. Furthermore, such mechanisms are not perfectly understood in any insect; although specific nervous system components have been studied in order to investigate adaptive behaviours of insects through visual, chemical and mechanical stimuli [28–30]. A useful finding from those works is that the insect brain can initiate and modulate flight via fiber neurons in response to stimulation of the visual, auditory, or wind receptors [31]. In addition, brain reconstruction of many insect species, such as Drosophila melanogaster [32], a honeybee [33], a desert locust [34] and the sphinx moth *Manducasexta* [35] has previously been described.

The rhinoceros beetle *T. dichotomus* is a large beetle that is easily raised across Asia. Due to its large size, the rhinoceros beetle is especially well suited as a candidate for the development of a MAV. In this study, we investigated the behavior of the beetle under electrical neural stimulation and the implementation of initiation, cessation and turning of the flight thereafter. In order to properly and precisely place the stimulation electrodes within the beetle's brain, we reconstructed a model of the brain of *T. dichotomus* using scanning electron microscopy and micro-computed tomography (CT) imaging. We then quantitatively measure the effects of electrical pulses applied to the brain and the basalar muscle of *T. dichotomus*. Four electrodes were implanted into the two optic lobes, the central complex (CC) in the brain and the ventral nerve cord in the posterior pronotum in order to implement flight control which includes flight initiation, flight direction and cessation. As stated earlier, neural stimulation was employed to trigger flight initiation and cessation as well as to alter the insect's flight orientation. Moreover, we observed beetle behavior in response to different combinations of electrical signals transmitted to the four electrodes. We visualized the beetle's flapping and investigated its flight characteristics. Based on the qualitative and quantitative analysis, we presented a method to control an insect for MAV.

2. Materials and methods

T. dichotomus is one of the largest insect species, weighing 6–10 g, which made it a suitable candidate for payload carriage.

2.1. Beetle anatomy

2.1.1. Scanning electron microscope (SEM) image of T. dichotomus brain. The whole brain was removed from the head exoskeleton prior to treatment. After beetle head dissection, the sample was placed in 4% paraformaldehyde. The tissue was rinsed of paraformaldehyde in cacodylate buffer (pH 7.2) followed by 10 min ethanol dehydration steps using 35%, 50%, 70%, 85%, 95%, and two times at 100% EtOH. The tissue was placed in Balzer's CPD030 critical point dryer and dried using the standard protocol (replacing the EtOH with liquid CO_2 and heating it to the critical point, followed by a slow release of the pressure). The dried sample was sputter coated with approximately 30 nm of thick gold/palladium coating using a sputter (Pelco Model 3) and then imaged in a SEM (Hitachi S-4700) at an accelerating voltage of 5 kV with a working distance of 12 mm and emission current of 16500 A.

2.1.2. Micro-CT. *T. dichotomus* was anesthetized with CO_2 and the head was cut off from the body. The head was subsequently put in a freezer at -5 °C for 30 min to be completely immobilized. The head capsule was mounted on the stage of the micro-CT machine. After the reconstruction from the raw images, the brain and optic lobes could be identified from the corresponding slice of the images. The optic lobes connect the brain to the compound eyes on both the left and right sides. Similarly, the female head was mounted on the micro-CT stage and scanned for 2 h and 37 min.
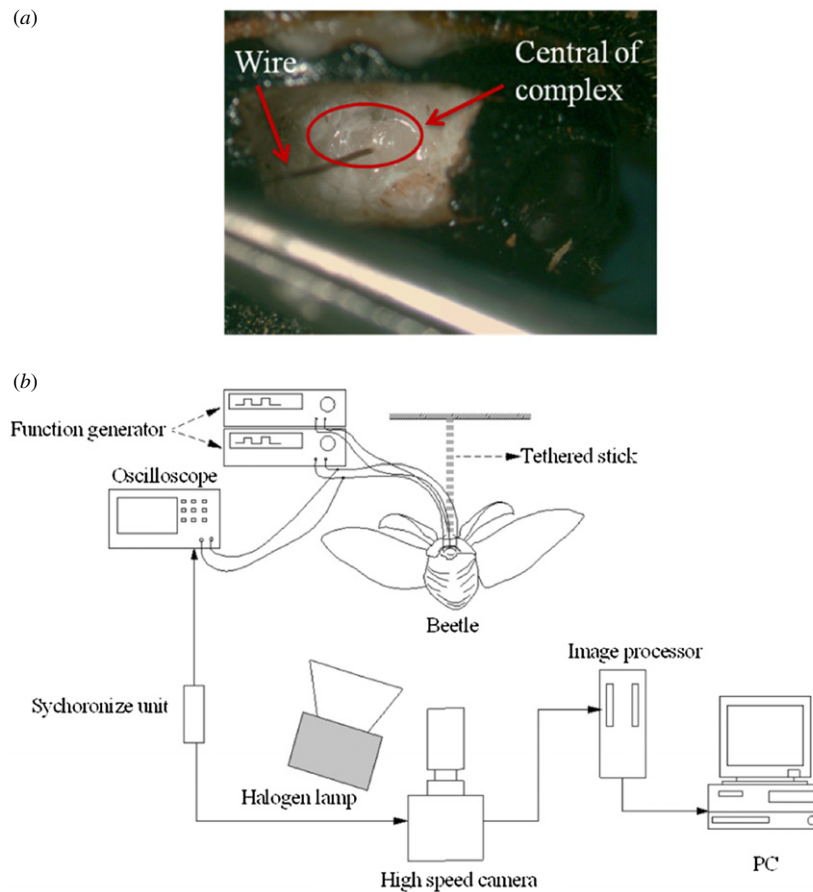
(*a*)

(*b*)

Figure 1. (*a*) A top view of an implanted electrode into CC. (*b*) The schematic of the experimental layout for the electrical stimulation.

The parameters for scanning were calibrated using an image of smaller pixel size in order to determine the minimum image resolution needed to provide sufficient details while avoiding long scan time. In figure 2(*b*), the brain and optic lobes can be clearly observed even after the pixel size was reduced to 5.52 μm. All of the images were taken using a high-resolution micro-CT (Skyscan1172) and its built-in reconstruction software.

2.2. Flight stimulation experiments

The beetles were kept on organic peat misted with 50% humidity and temperature of 25 °C. The beetles were starved for 24 h before the stimulation experiments. To anesthetize the beetles, each beetle was placed into a chamber with carbon dioxide gas for at least 30 s. To determine the specific and precise location for stimulation, the cuticle and tissues obstructing visibility of the brain from entry point are removed prior to electrode implantation. A micromanipulator and a very small probe ($\sim$50 $\times$ 15 μm^2) are used to cut a shallow hole in the brain sheath (figure 1(*a*)). A small (80 μm) double-braided wire is then attached to the manipulator and carefully inserted into the hole.

After obtaining information about the dimensions and morphology of the brain of *T. dichotomus* using the SEM, we were able to determine the optimal size of the electrode. Moreover, the three-dimensional morphology of the brain in the head capsule reconstructed using the micro-CT images

allowed us to determine the position at which the electrodes should be implanted for neural stimulation. Using optical microscope imaging, we can verify the position of the electrodes post-implantation (figure 1(*a*)).

A needle was used to pierce four small holes through the beetle's cuticle: at the interior edge of the left and right compound eyes for optic lobe, at the center complex of the brain and at ventral nerve cord in the center of the posterior of pronotum. In order to test the muscle response with a potential, a hole was made midway between the sternum and notum of the mesothorax in order to access the direct flight muscles. For response testing, four steel wires (working as electrodes) were implanted into the small holes. A schematic diagram of the experimental apparatus is shown in figure 1(*b*). Two halogen lamps with a power of 1 kW were placed at appropriate positions to illuminate the region. The high-speed camera lens was connected to a camera and computer, while Photron FASTCAM Viewer software® was used to capture images and control the high-speed camera system. The beetle was hung by a wooden applicator stick fixed on its head using super glue. The position of the beetle was oriented perpendicularly to the camera lens. The beetle's wing motion was captured with a high-speed camera at 2000 frames per second (fps) in 1 μs shutter time and 1024 $\times$ 1024 pixels screen resolution for the front view. The wires were connected to two function generators (Agilent, 33220 A). The oscilloscope was used to examine the characteristics of the applied potential. The high-speed camera was synchronized with the oscilloscope in order
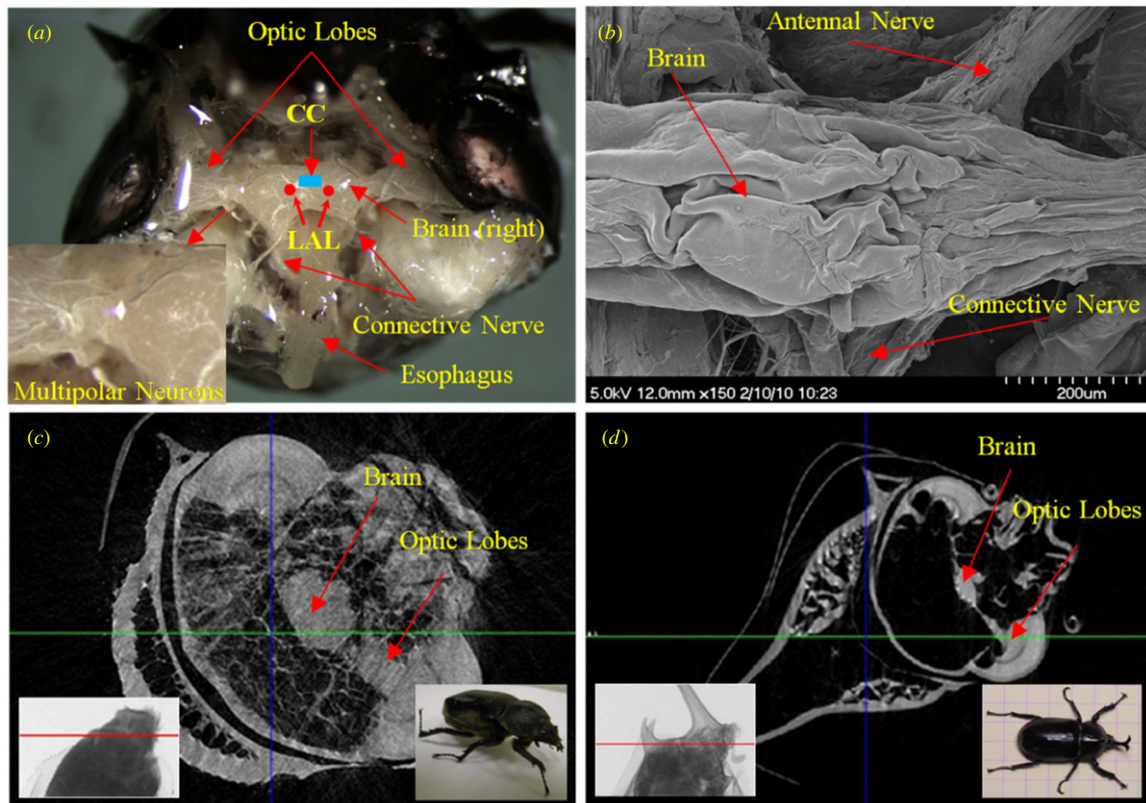
Figure 2. The brain anatomy of *T. dichotomus*. (*a*) Anatomical preparation of the brain of a *T. dichotomus* adult male (anterio-dorsal view after removal of the anterior head capsule). The approximate location of the CC and the LAL are indicated. (*b*) SEM of *T. dichotomus* brain at 200 μm in-plane resolution. (*c*, *d*) Micro-CT images of the head of a *T. dichotomus* adult female and male. The inset image to the left shows the plane of the micro-CT scan. The inset image to the right shows the adult beetle.

to examine the flight response with the state of the applied potential. The response time of the beetle was given using by—audio recording. The kinematics data were filtered with a Butterworth filter at a cutoff frequency of 160 Hz, nearly four times greater than the flapping frequency (35–40 Hz). In brief, we used four female beetles to capture wing kinematics. The flapping angle was defined as the angle between the line that joins the wing base to wing tip and the horizontal axis. The flapping angles were manually calculated using the AutoCAD software. The neural stimulation was employed first. Then we implanted electrodes into direct muscles to carry out muscular stimulation. Each beetle was filmed to record two movies—with neural stimulation and two movies with muscular stimulation. In total, around 88 wing beats in muscular stimulation and 88 wing beats in neural stimulation from four female beetles were used to measure flapping angle.

3. Result

3.1. Brain morphology

The head and thorax of male *T. dichotomus* were dissected in order to examine the basalar muscular and nervous system. The male beetle possesses a head capsule that is softer than that of a female; other than that, there are no significant differences between males and females in regard to brain morphology [36]. We carefully removed the epicranium from the region between the compound eyes and antennae, and

then removed the muscles necessary to reveal the brain, as shown in figure 2(*a*). This dissection provided a comprehensive view of the *T. dichotomus* brain. Additionally, the image displayed other parts of the brain such as the optic lobe and esophagus. The protocerebrum had a large spherical structure (figure 2(*a*)), which hosts the mushroom bodies and CC [35]. The circumesophageal connectives link the subesophageal ganglion in the head with the ventral nerve cord in the thorax and abdomen. In the tubular esophagus, signals from the brain pass to the nerve cord via a few hundred descending axon fibers [37].

A SEM was used to obtain the dimensions and morphology of the brain of *T. dichotomus*. Figures 2(*a*) and (*b*) show the antennal nerves. Furthermore, the brain and optic lobe sites for electrode implantation were identified. Brain size was estimated from the SEM images to be approximately 446 μm in diameter and 1640 μm in length. Electrode size was chosen to correspond to these measurements. Moreover, the micro-CT images (figures 2(*c*) and (*d*)) provided a three-dimensional morphology of the brain in the head capsule, which allowed us to determine the position at which the electrodes should be implanted for neural stimulation.

Previous studies have reported the brain structure of an insect and functions for flight control. CC is a group of neuropil in the center of the insect brain in multimodal sensorimotor integration [38]. The CC is composed of four major sub-units: the upper and lower divisions of the central body (CBU, CBL), the protocerebral bridge and the paired

Table 1. Control of flight initiation by electrical stimulation of the two optic lobes of *T. dichotomus*.

Samples	1	2	3	4	5	6	7	8	9	10
Mb (g)	3.96	4.67	4.65	3.98	4.35	5.25	4.58	5.12	4.86	4.87
Hind wing length (mm)	43.86	44.35	42.23	43.67	42.26	47.87	45.3	48.11	45.56	44.81
Elytron length (mm)	24.15	24.92	25.21	24.12	24.73	26.19	25.1	25.98	25.56	25.27
Amplitude (V)	1.3	3.2	2.5	3.5	2.9	3.9	2.3	3.7	2.2	3.6
Stimulation time for continuous flight (s)	22.53	24.32	24.6	20.79	21.16	23.47	25.02	23.53	24.36	20.85
Response time for initiation (s)	9.08	8.72	4.29	2.38	1.85	2.67	6.14	1.43	1.01	10.93

nodule [39]. Structural CC mutants in *Drosophila* showed defects in directional control flight [40]. The lateral accessory lobe (LAL) is a neuropil area in the protocerebrum of the brain. A role of the CC in flight control might be accomplished via pathways through the LAL [41]. The CC responded to visual, chemical, mechanical stimuli [42] and electrical stimulation [43]. The optic lobe consists of three neuropils: the lamina, medulla, and lobula complex [44]. The electrical signal of the optic lobe toward the central brain apparently plays important roles in locomotor rhythm [45]. The movement of the flight muscles could be produced by the stimulation of the central nervous system anywhere from brain to the abdominal cord [46]. Therefore, for the beetle in this study, the optic lobes, CC and ventral nerve cord may play a significant role to flight control. We selected and implanted four electrodes into those positions in the beetle's head.

3.2. Initiation and cessation of flight

Electrical activity was observed between the optic lobes, which are connected to the brain through the efferent neuron [47]. Action potentials were found to be localized in the origin, arising from the deeper part of the second synaptic region, and in some cases also from the third synaptic region of the optic lobe [48]. Electrical activity between the two optic lobes usually develops spontaneously, showing regular sinusoidal waves where it has been described [48]. In this study, we observed natural sinusoidal waves between the optic lobes which had a 1 Hz frequency for *T. dichotomus* (see movie S1, available from http://stacks.iop.org/BB/7/036021/mmedia). The bipolar electrodes in the optic lobes generated the shocks, which simultaneously elicited one-to-one junction potential in all dorsal longitudinal muscles [49].

At first, we attempted to control flight initiation and cessation using electrical stimulation between the four electrodes implanted in the two optic lobes, the brain's CC and the ventral nerve cord in the posterior pronotum. We implanted the electrode into the posterior pronotum where the ventral nerve cord runs across for cessation of the flight. Nerve cells are linked together and transmit information as electrical current to other nerve cells or muscle cells. We speculated that the transmission of the signal through the nerve system to make fly would be disturbed due to the externally applied electrical potential. By applying the electrical stimuli between the optic lobe and the pronotum, we could demonstrate the cessation of the flight. Various frequencies, amplitudes and wave forms were employed between the two electrodes in order to identify the optimal signal. Ten active female beetles were chosen for the experiment primarily because female beetles exhibit more active flight abilities than male beetles [50].

When attempting to control flight initiation, we found that only the rectangular wave form was able to elicit the initiation of beetle flight: eight of the ten beetles initiated flight with alternating positive and negative potential pulses, while the other two beetles started their flights with positive pulses. The optimal frequency was 1 Hz, which is identical to the frequency of the sinusoidal wave's electrical activity between the optic lobes, indicating that the applied rectangular pulse should be synchronized with the natural electrical signal between the optic lobes. Generally, coleopteran insects possess asynchronous flight muscles which oscillate under indirect control [51]. Duch and Pflüger found that neuron innervated flight muscle triggers flight with frequencies between 0.1 and 1 Hz for a locust, which has a flapping frequency of around 25 Hz [52]. Similarly, because the beetle possesses asynchronous flight muscles, the flapping frequency of the beetle is 35 Hz, which is much greater than the optimal initiation frequency of 1 Hz. It should be noted that in these species, motor neurons to the flight muscles release at much lower frequencies than the wing oscillation frequencies [53]. The asynchronous operation has been favored by evolution in flight systems of different insect groups because it generates greater output at the high contraction frequency of flight [53].

Table 1 shows the response time for flight initiation and duration of the stimulation for continuous flight even after turning off the stimulation. The optimal duty cycle was 50% for eight beetles and 20% for two beetles. The duty cycle was defined by the ratio of the positive pulse time to one cycle duration time. The threshold amplitude of the potential varied from 1.3 to 3.9 V. When the electrical potential was lower or higher than the threshold voltage, the beetles did not fly and the body just contracted due to the electrical shock. When the potential frequency was less than 1 Hz, beetles exhibited interrupted flight. At positive pulses, beetles repeated the initiation of flight; whereas, at negative pulses, beetles ceased flight (movie S2, available from http://stacks.iop.org/BB/7/036021/mmedia). Beetles were able to continue stable flight at 1 Hz even after the electrical potential was turned off (movie S2, available from http://stacks.iop.org/BB/7/036021/mmedia). However, when the duration of the applied potential was less than 20 s, all beetles ceased flight when the potential was turned off (table 1). When the duration time was longer than around 25 s, beetles continued flight even after the potential was turned off.

We also investigated three different methods for flight cessation. First, we applied an electrical pulse to both optic lobes with a specific frequency or amplitude
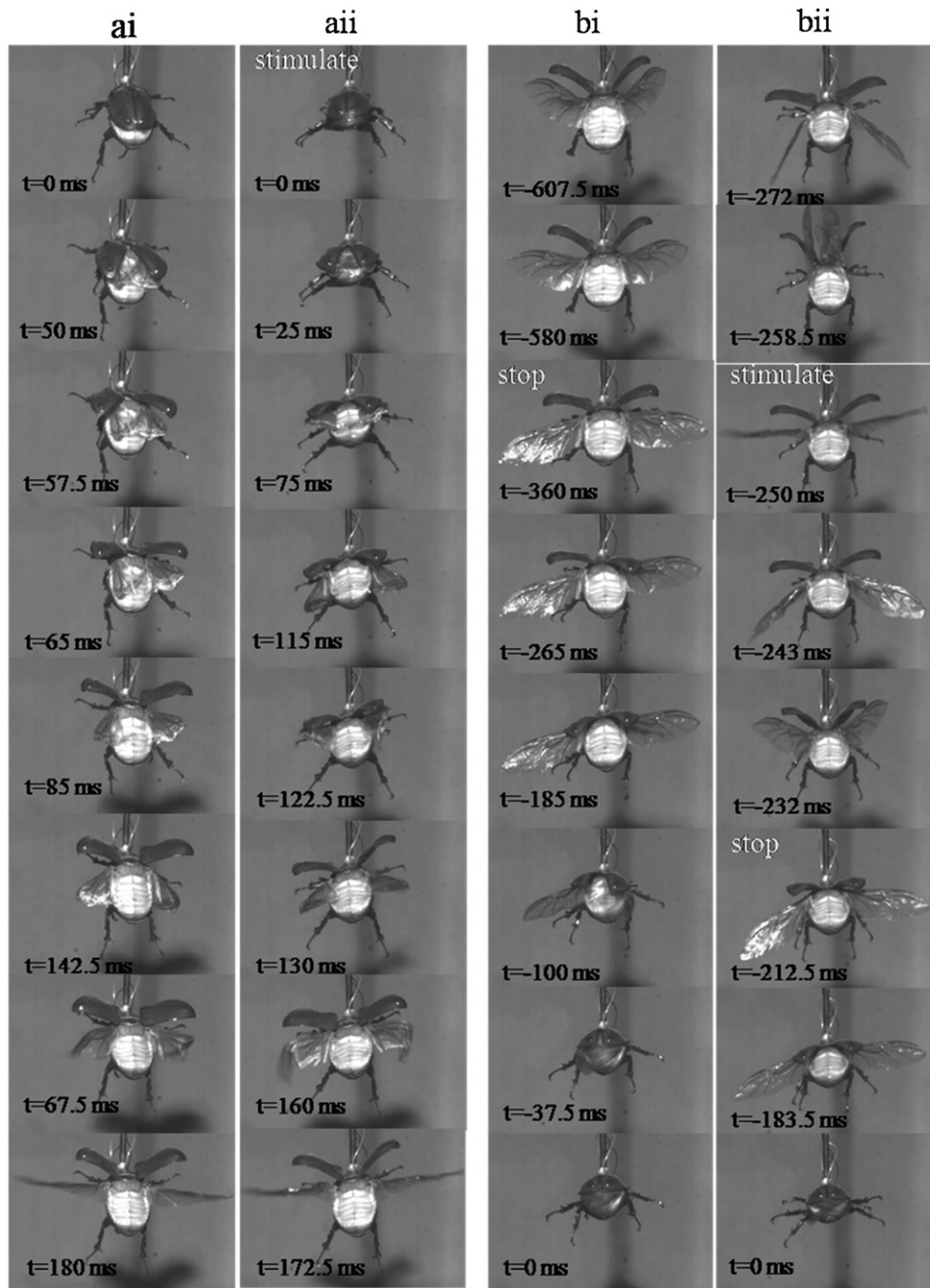
Figure 3. Sequential images of the opening and closing motions of the elytra and unfolding and folding motion of the hind wing. (*a*-i) Natural opening and unfolding motion. (*a*-ii) Electrically stimulated opening and unfolding motion. (*b*-i) Natural closing and folding motion. (*b*-ii) Electrically stimulated closing and folding motion.

to end beetle flight. When the frequency increased to 11 Hz, the beetle ceased flight (movie S3, available from http://stacks.iop.org/BB/7/036021/mmedia). Second, if the amplitude of the applied pulse was increased to more than 4 V, the cessation of flight was also achieved. In addition to these two ways, flight was stopped by application of the electrical stimulation pulse between either side of the optic lobe and the ventral nerve cord, or between the CC and the ventral nerve cord (movie S3, available from http://stacks.iop.org/BB/7/036021/mmedia).

To gain a clear understanding of artificially induced flight behavior as it relates to natural flight, we visualized the detailed motions of flight initiation and cessation and compared those findings to the motions of natural flight without electrical stimulus. Four electrodes were implanted into the two optic lobes, the CC and the ventral nerve cord in the posterior pronotum. The alternating electrical pulses with amplitude of 3.2 V, frequency of 1 Hz and duty cycle of 20% were applied to four electrodes implanted into the left and right optic lobes, the CC and the ventral nerve cord. Figure 3 shows a series of photographs recorded at 2000 fps from the posterior of the insect. All of the tested beetles initiated flight during the positive pulses.
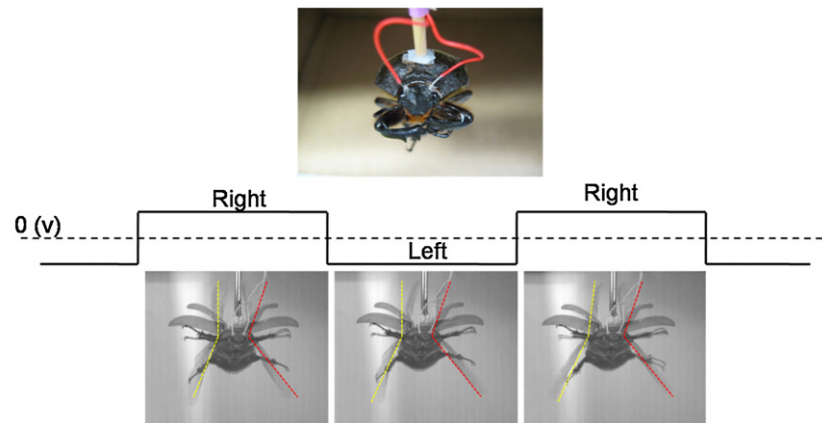
Figure 4. Tethered flight stimulation experiment with two electrodes implanted into the left and right optic lobes of *T. dichotmus*. The sequence images are recorded though a 2000 Hz high-speed video camera assembled at a front view. A rectangular wave form of 1 Hz, 3.5 V and 50% duty cycle was sent to the electrodes (one electrode was specified as a counter electrode). In the first 500 ms of the cycle, the positive pulse was from the right electrode which caused the flapping angle of the right wing to be reduced. Afterward, the flapping angle of the left wing was reduced following a positive pulse to the left electrode.

In this study, we described the kinematics of the elytra openings and closings for a *T. dichotomus*. The elytra were released at $t = 50$ ms, rotated forward, and were fully elevated at $t = 85$ ms during the natural opening period (figure 3(*a*-i)). However, during electrical stimulation, nearly twice as much time was used to fully open the elytra. In particular, during electrical stimulation, the beetle experienced difficulty in opening the elytra. As shown in figure 3(*a*-ii), the elevation angle was smaller than that of the natural opening during $t = 75$–122.5 ms (see movie S4, available from http://stacks.iop.org/BB/7/036021/mmedia). It has been reported previously from other beetle studies that the forward movement of the pronotum and depression of the metathorax with respect to the mesothorax unlock the elytra [54]. However, our observations indicated that the elytra were driven by the elytron muscle. More importantly, these observations suggested that motor neurons in the elytral muscle are connected to the brain. The unfolding motion of the hind wings was triggered by actuation of the basalar muscle in the abdomen and the mesothorax [55]. Notably, the duration time observed for full unfolding and the flight posture was similar between both the natural and stimulated cases (figures 3(*a*-i) and (*a*-ii)).

During natural flight cessation, the duration time taken for flapping to slow down and stop was 240 ms (figure 3(*b*-i)). However, we observed that the beetle ceased flight immediately after the application of an electrical stimulus between the optic lobe and the pronotum (37.5 ms). During the wing folding process, elastic energy is stored in resilin, a rubber-like substance [55]. The time required to complete hind wing folding and elytral closing was much faster when electrically stimulated (212.5 ms) than occuring naturally (360 ms). Further evidence for motor neuron activation of the elytral muscle is shown in figures 5(*b*-i) and (*b*-ii). When the beetle completely ceased flapping, the elevation angle of the elytra in the natural case was hingher (at $t = -360$ ms) than when the beetle was stimulated (at $t = -212.5$ ms) (see movie S4, available from http://stacks.iop.org/BB/7/036021/mmedia). In

a previous study, Frantsevich [56] concluded that the elevation of the prothorax was the direct and main mechanism of elytral closing. In contrast, the current observation implies that the closing motion of the elytra might be driven by the beetle's muscle, which is controlled by motor neurons. In the response potential, the average time between the start of the electrical stimulus pulse to the beginning of flapping was 4.92 s (range 1.01–10.93 s; see table 1).

The flight initiation was elicited when the external potential was applied between the two electrodes implanted into optic lobes. To obtain more details of the flight behavior under this condition, alternating positive potential pulses (1 Hz) were applied to the left and right optic lobes in weak tethered flight experiments (movie S5, available from http://stacks.iop.org/BB/7/036021/mmedia). The beetle turned left or right accordingly in response to positive or negative pulses, respectively. From high-speed camera images of a tethered flight stimulation experiment (figure 4), the alternating pulse potential of the left and right electrodes in the optic lobe induced an alternating reduction of the flapping angle on one side of the insect. This reduction induced the beetle to turn left and right alternately. When we stopped applying the electrical signal, the beetle flapped steadily. This indicates that the beetle could not achieve stable flight due to continuously alternating turns during flight when only two electrodes are implanted in the optic lobes; therefore, four electrodes must be implanted in order to achieve fully controllable stable flight.

3.3. Turning flight

We tried to implement the turning flight using four electrodes' stimulation and studied wing flapping behavior during the turning. Similarly to the method used in the electrical muscles' stimulation (used in [23]), the turning flight was also analyzed when the electrical stimulus was applied to the electrodes implanted into the right basalar muscle and ventral nerve cord in the posterior pronotum (counter electrode) (figure 5(*a*)). The depth of the inserted wire electrodes was equal to the
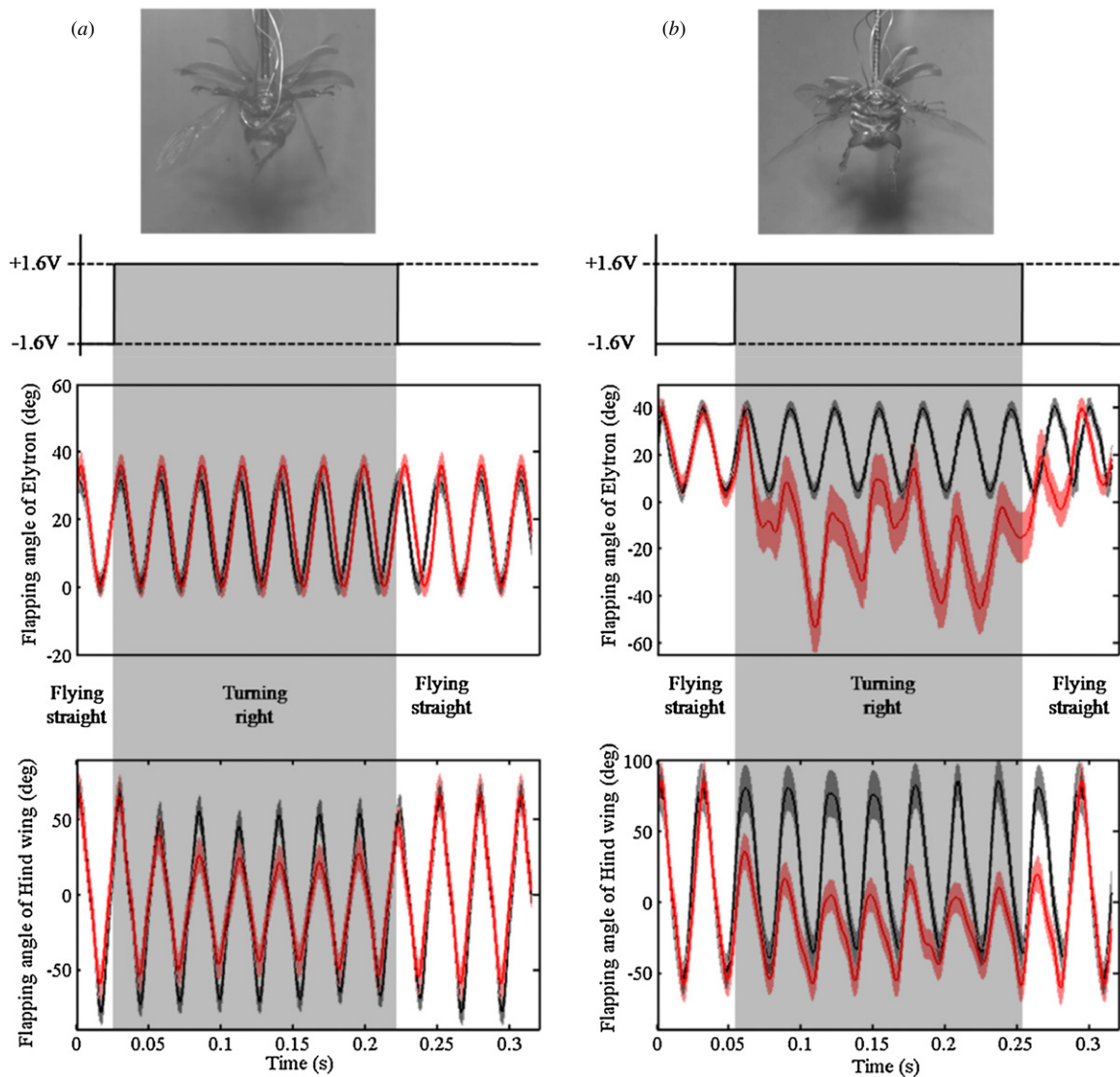
Figure 5. Neuronal and muscular electrical stimulations of induced (or artificially controlled) beetle flight. Images are recorded through a 2000 Hz high-speed video camera from a front view. (*a*) The flapping angle of the hind wings and elytra when applying the electrical potential between the right muscle and pronotum. (*b*) The flapping angle of the hind wings and elytra when applying the electrical potential between the brain and the right optic lobe. The red and black lines represent the flapping angles over time of the right and the left wings, respectively. The shaded region around those red and black lines displays the instantaneous standard deviation. The shaded bar corresponds to the positive pulse period.

length of the muscle fibers. The orientation of the electrodes followed the direction of the fibers. In this study, we suggested that the turning flight could be implemented more effectively by using only neural stimulation via the four electrodes. To make a right turn, the electrical signal was applied to the wire electrodes inserted into the right optic lobe and CC in the brain (counter electrode) (figure 5(*b*)). The potential stimulus had amplitude of 3.2 V, frequency of 1 Hz and duty cycle of 20%. The size of the electrode was 80 μm in diameter. This potential condition elicited the initiation of beetle flight (in the initiation and cessation flight part). We evaluated flight characteristics by measuring the flapping angle of the hind wing and the elytra during stimulation.

Figure 5 illustrates the variation of the flapping angle of the hind wings and the elytra during electrical stimulation versus natural flight. Figure 5 compares the turning behaviors according to the muscle stimulation and the neural stimulation.

When the muscle was stimulated, the flapping angles of the elytra were constant during positive and negative pulse potentials. However, considerable differences in the flapping angle of the hind wings during muscular stimulation were observed, which made the turning (figure 5(*a*)). The flapping angle of the one stimulated hind wing was decreased throughout the positive pulse period; whereas, the other hind wing exhibited a negligible decrement and flapped steadily. At the beginning of the positive potential pulse, the original pronation phase of the right hind wing still commenced, which could be due to its initial momentum. In the subsequent stroke, the flapping angle of the right hind wing reduced from $27.3 \pm 13.8°$ at upstroke to $9.9 \pm 10.7°$ ($N = 4$) at downstroke in comparison to the negative pulse. The flapping angle was reduced by $47.5 \pm 17.3\%$ over the total stroke during the midpoint of the positive pulse period. The angle variation of the right hind wing was slightly symmetric during the

positive pulse period. At the beginning of the negative pulse stage, the right hind wing recovered immediately from squeeze commenced normal flapping. This phenomenon indicates that the potential strongly evoked the shrinking of only the direct muscle. Furthermore, the results indicated that the muscle of the hind wing operated independently of the elytra muscle. The small change in flapping angle of the left hind wing could be affected by the vibration of the muscle system.

When the electrical signal was applied to the wire electrodes inserted into the optic lobe and CC in the brain, the flapping angles of both the elytron and the hind wing as a result of one simulated optic lobe decreased during the positive potential pulse (figure 5(*b*)) (movie S6, available from http://stacks.iop.org/BB/7/036021/mmedia). In particular, the right elytron exhibited disorderedly beating throughout the positive pulse, as illustrated by the red line in figure 5(*b*). When the positive pulse stage commenced, the elytron flapped below the horizontal plane, generating a negative flapping angle and continued fluctuating during the positive pulse period. In contrast, no disturbances were observed at the left elytron, as shown in figure 5(*b*). While the right hind wing was going up, the right basalar muscle contracted; therefore, it did not reach the original pronation. Consequently, the flapping angle of the right hind wing decreased by $48.8 \pm 11.0°$ ($N = 4$) at upstroke in comparison with the previous stroke. The overall flapping angle of the hind wing under neural stimulation was smaller by $20.5 \pm 17.3\%$ ($N = 4$) than those under muscular stimulation. Because of the strong effect of neural stimulation, the reduction of the flapping angle of the elytron and the hind wing was maintained during one more stroke even after switching the pulse to negative (figure 5(*b*)). It seems that the effect of neural stimulation on direct muscle is stronger than that of muscle stimulation alone.

Based on our study for flight behavior under neuronal stimulation (figure 5(*b*)), we were able to demonstrate advanced flight turning control by stimulating only the brain using four electrodes. We used four thin wire electrodes (100 μm) and implanted these in the ventral nerve cord in the pronotum, CC and the left and right optic lobes. A small camera (model VID 004 color) was attached to the beetle's head (movie S7, available from http://stacks.iop.org/BB/7/036021/mmedia) capturing the images. The beetle's flight direction changed when one side of the optic lobe was electrically stimulated. The beetle's flight direction remained stable when one side of optic lobe and CC was electrically stimulated. A total of seven beetles were employed in the experiment. All of the beetles consistently exhibited left and right turns following neural stimulation on one side of the optic lobe.

4. Discussion and conclusion

In this study, we reported the results of the effect of neuronal electrical stimulation on initiation, duration and cessation of rhinoceros beetle flight, and demonstrated control of turning. Specifically, we found neuronal fibers and connections linking one side of the optic lobe to the subesophagueal ganglion in the head. This observation provides important new information

for hypotheses of flight control in beetles. Our results suggest that the neural circuitry between the optic lobes transmits a rate-driven signal from the visual system in complex eye side to the wings muscle side for voluntary turns [57]. We provided evidence to distinguish the important differences between neuronal and muscular flight stimulation. We found that in the neural potential stimulation, both the hind wing and the elytron were suppressed. The reduction of the flapping angle of the hind wing during neural stimulation was higher than that which occurred during muscular stimulation. Moreover, the hind wings during neural stimulation responded faster and more strongly than during muscular stimulation. The beetle possesses elytra, which contribute to aerodynamic forces in forward flight [16]. The smaller flapping angle of the hind wing and elytra would produce higher yaw torque during the turning motion. These observations showed that the neural stimulation was more effective than muscular stimulation for turning control.

A current was generated between the electrodes in the optic lobe and central complex to perhaps elicit segmental interneuron. The signal was then transferred through the specific connection neurons (as shown in figure 2(*a*)) to the flight motor neurons in one side of the thoracic and abdominal system. This suggests that applying an electrical stimulus to the electrodes implanted on the optic lobe and central complex in the brain would induce the flapping of the hind wing and elytra. We also found that muscular stimulation would affect only the hind wing, indicating that the hind wing muscle operates separately from the elytra muscle. This finding emphasizes the need for further studies to explore the role of the neuron system underlying flight control in beetles. In addition, the quantified sequence of initiation and cessation motions indicated that elytra were driven by its muscle and motor neuron.

Our results coincide with previous results highlighting the exciting potential for large-bodied insects to be manipulated as MAVs. Our findings show that whenever we send the stimulus potential between the pronotum and one side of the optic lobe or the middle brain, flight cessation can be controlled. We also demonstrated that neural stimulation was a stronger influence than muscle stimulation. It offered more control during turning than muscular stimulation. In addition, by applying electrical signals between two electrodes implanted into optic lobes, the beetle could not fly stably, resulting in alternating left and right turns. By applying electrical signals between four electrodes implanted into optic lobes, central complex of the brain and central nerve cord in pronotum, we were able to precisely control the direction of beetle flight in a very stable manner. Based on this qualitative and quantitative analysis, we proposed the manner to control insect-MAV by using only neural stimulation.

References

[1] Bozkurt A, Paul A, Pulla S, Ramkumar A, Blossey B, Ewer J, Gilmour R and Lal A 2007 Microprobe microsystem platform inserted during early metamorphosis to actuate insect flight muscle *IEEE 20th Int. Conf. on Micro Electro Mechanical Systems* pp 405–8

[2] Holzer R and Shimoyama I 1997 Locomotion control of a bio-robotic system via electric stimulation *IEEE Conf. on Intelligent Robots and Systems* vol 3 pp 1514–9

[3] Lemmerhirt D F, Staudacher E M and Wise K D 2006 A multitransducer microsystem for insect monitoring and control *IEEE Trans. Biomed. Eng.* **53** 2084–91

[4] Talwar S K, Xu S, Hawley E S, Weiss S A, Moxon K A and Chapin J K 2002 Behavioural neuroscience: rat navigation guided by remote control *Nature* **417** 37–38

[5] Dickinson M 2006 Insect flight *Curr. Biol.* **16** R309–14

[6] Dudley R 2002 *The Biomechanics of Insect Flight: Form, Function, Evolution* (Princeton, NJ: Princeton University Press)

[7] Dickinson M H, Lehmann F-O and Sane S P 1999 Wing rotation and the aerodynamic basis of insect flight *Science* **284** 1954–60

[8] Birch J M and Dickinson M H 2001 Spanwise flow and the attachment of the leading-edge vortex on insect wings *Nature* **412** 729–33

[9] Srygley R B and Thomas A L R 2002 Unconventional lift-generating mechanisms in free-flying butterflies *Nature* **420** 660–4

[10] Hedrick T L, Cheng B and Deng X 2009 Wing beat time and the scaling of passive rotational damping in flapping flight *Science* **324** 252–5

[11] Ristroph L, Bergou A J, Ristroph G, Coumes K, Berman G J, Guckenheimer J, Wang Z J and Cohen I 2010 Discovering the flight autostabilizer of fruit flies by inducing aerial stumbles *Proc. Natl Acad. Sci. USA* **107** 4820–4

[12] Wood R J 2008 The first takeoff of a biologically inspired at-scale robotic insect *IEEE Trans. Robot.* **24** 341–7

[13] Kim W-K, Ko J H, Park H C and Byun D 2009 Effects of corrugation of the dragonfly wing on gliding performance *J. Theor. Biol.* **260** 523–30

[14] Lee Y, Yoo Y, Kim J, Widhiarini S, Park B, Park H C, Yoon K J and Byun D 2009 Mimicking a superhydrophobic insect wing by argon and oxygen ion beam treatment on polytetrafluoroethylene film *J. Biol. Eng.* **6** 365–70

[15] Hiroto T and Isao S 2010 Forward flight of swallowtail butterfly with simple flapping motion *Bioinspir. Biomim.* **5** 026003

[16] Le T Q, Byun D, Saputra P, Ko J H, Park H C and Kim M 2010 Numerical investigation of the aerodynamic characteristics of a hovering Coleopteran insect *J. Theor. Biol.* **266** 485–95

[17] Nguyen Q V, Truong Q T, Park H C, Goo N S and Byun D 2010 Measurement of force produced by an insect-mimicking flapping-wing system *J. Biol. Eng.* **7** S94–102

[18] Nguyen Q V, Park H C, Goo N S and Byun D 2010 Characteristics of a beetle's free flight and a flapping-wing system that mimics beetle flight *J. Biol. Eng.* **7** 77–86

[19] Paul A, Bozkurt A, Ewer J, Blossey B and Lal A 2006 Surgically implanted micro-platforms in *Manduca sexta Solid State Sensor and Actuator Workshop (Hilton Head Island)* pp 209–11

[20] Taylor G K 2001 Mechanics and aerodynamics of insect flight control *Biol. Rev.* **76** 449–71

[21] Bozkurt A, Lal A and Gilmour R 2008 Electrical endogenous heating of insect muscles for flight control *IEEE Conf. on Engineering in Medicine and Biology* pp 5786–9

[22] Chung A J and Erickson D 2009 Engineering insect flight metabolics using immature stage implanted microfluidics *Lab on a Chip* **9** 669–76

[23] Bozkurt A, Gilmour R F and Lal A 2009 Balloon-assisted flight of radio-controlled insect biobots *IEEE Trans. Biomed. Eng.* **56** 2304–7

[24] Sato H, Berry C W, Peeri Y, Baghoomian E, Casey B E, Lavella G, VandenBrooks J M, Harrison J and Maharbiz M M 2009 Remote radio control of insect flight *Front. Integr. Neurosci.* **4** 12

[25] Sato H, Berry C W and Maharbiz M M 2008 Flight control of 10 gram insects by implanted neural stimulators *Solid State Sensor Actuator Workshop (Hilton Head Island)* pp 90–91

[26] Daly D C, Mercier P P, Bhardwaj M, Stone A L, Aldworth Z N, Daniel T L, Voldman J, Hildebrand J G and Chandrakasan A P 2010 A pulsed UWB receiver SoC for insect motion control *IEEE J. Solid-State Circuits* **45** 153–66

[27] Tsang W M, Stone A L, Aldworth Z N, Hildebrand J G, Daniel T L, Akinwande A I and Voldman J 2010 Flexible split-ring electrode for insect flight biasing using multisite neural stimulation *IEEE Trans. Biomed. Eng.* **57** 1757–64

[28] Gray J R, Pawlowski V and Willis M A 2002 A method for recording behavior and multineuronal CNS activity from tethered insects flying in virtual space *J. Neurosci. Methods* **120** 211–23

[29] Heinze S and Homberg U 2007 Maplike representation of celestial E-vector orientations in the brain of an insect *Science* **315** 995–7

[30] Ritzmann R, Ridgel A and Pollack A 2008 Multi-unit recording of antennal mechano-sensitive units in the central complex of the cockroach, Blaberus discoidalis *J. Comp. Physiol.* A **194** 341–60

[31] Frye M A and Dickinson M H 2004 Closing the loop between neurobiology and flight behavior in Drosophila *Curr. Opin. Neurobiol.* **14** 729–36

[32] Rein K, Zöckler M, Mader M T, Grübel C and Heisenberg M 2002 The Drosophila standard brain *Curr. Biol.* **12** 227–31

[33] Brandt R, Rohlfing T, Rybak J, Krofczik S, Maye A, Westerhoff M, Hege H-C and Menzel R 2005 Three-dimensional average-shape atlas of the honeybee brain and its applications *J. Comp. Neurol.* **492** 1–19

[34] Kurylas A, Rohlfing T, Krofczik S, Jenett A and Homberg U 2008 Standardized atlas of the brain of the desert locust *Cell Tissue Res.* **333** 125–45

[35] El Jundi B, Huetteroth W, Kurylas A E and Schachtner J 2009 Anisometric brain dimorphism revisited: implementation of a volumetric 3D standard brain in Manduca sexta *J. Comp. Neurol.* **517** 210–25

[36] Dreyer D, Vitt H, Dippel S, Goetz B, El Jundi B, Kollmann M, Huetteroth W and Schachtner J 2009 Ribolium castaneum: a tool to study metamorphic development and adult plasticity *Front. Syst. Neurosci.* **5** 12

[37] Jan W and Barbara W 2006 Multimodal sensory integration in insects—towards insect brain control architectures *Bioinspir. Biomim.* **1** 63

[38] Boyan G S and Reichert H 2011 Mechanisms for complexity in the brain: generating the insect central complex *Trends Neurosci.* **34** 247–57

[39] Heinze S and Homberg U 2008 Neuroarchitecture of the central complex of the desert locust: intrinsic and columnar neurons *J. Comp. Neurol.* **511** 454–78

[40] Roland S 2002 The central complex and the genetic
dissection of locomotor behaviour *Curr. Opin. Neurobiol.*
12 633–8

[41] Homberg U 1994 Flight-correlated activity changes in neurons
of the lateral accessory lobes in the brain of the locust
Schistocerca gregaria *J. Comp. Physiol.* A **175** 597–610

[42] Heinze S and Homberg U 2007 Maplike representation of
celestial E-vector orientations in the brain of an insect
Science **315** 995–7

[43] Bender J A, Pollack A J and Ritzmann R E 2010 Neural
activity in the central complex of the insect brain is linked
to locomotor changes *Curr. Biol.* **20** 921–6

[44] Sbita S J, Morgan R C and Buschbeck E K 2007 Eye and optic
lobe metamorphosis in the sunburst diving beetle,
Thermonectus marmoratus (Coleoptera: Dytiscidae)
Arthropod Struct. Dev. **36** 449–62

[45] Tomioka K and Abdelsalam S 2004 Circadian organization in
hemimetabolous insects *Zool. Sci.* **21** 1153–62

[46] Wilson D M 1961 The central nervous control of flight in a
locust *J. Exp. Biol.* **38** 471–90

[47] Tomioka K, Nakamichi M and Yukizane M 1994 Optic lobe
circadian pacemaker sends its information to the
contralateral optic lobe in the cricket *J. Comp. Physiol.* A
175 381–8

[48] Burtt E T and Catton W T 1960 The properties of single-unit
discharges in the optic lobe of the locust *J. Physiol.*
154 479–90

[49] Gordon S and Dickinson M H 2006 Role of calcium in the
regulation of mechanical power in insect flight *Proc. Natl
Acad. Sci. USA* **103** 4311–5

[50] Hongo Y 2003 Appraising behaviour during male-male
interaction in the Japanese horned beetle trypoxylus
dichotomus septentrionalis (Kono) *Behaviour*
140 501–17

[51] Josephson R, Malamud J and Stokes D 2000 Power output by
an asynchronous flight muscle from a beetle *J. Exp. Biol.*
203 2667–89

[52] Duch C and Pflüger H J 1999 DUM neurons in locust flight: a
model system for amine-mediated peripheral adjustments to
the requirements of a central motor program *J. Comp.
Physiol.* A **184** 489–99

[53] Josephson R, Malamud J and Stokes D 2000 Asynchronous
muscle: a primer *J. Exp. Biol.* **203** 2713–22

[54] Frantsevich L, Dai Z, Wang W Y and Zhang Y 2005 Geometry
of elytra opening and closing in some beetles (Coleoptera,
Polyphaga) *J. Exp. Biol.* **208** 3145–58

[55] Haas F and Beutel R G 2001 Wing folding and the functional
morphology of the wing base in Coleoptera *Zoology*
104 123–41

[56] Frantsevich L 2010 Indirect closing of the elytra in a
cockchafer, Melolontha hippocastani F. (Coleoptera:
Scarabaeidae) *J. Exp. Biol.* **213** 1836–43

[57] Dickinson M H 2005 The initiation and control of rapid flight
maneuvers in fruit flies *Integr. Comp. Biol.* **45** 274–81